



ELSEVIER

Note

A redetermination of the crystal and molecular structure of maltitol (4-*O*- α -D-glucopyranosyl-D-glucitol)Arie Schouten ^{a,*}, Jan A. Kanters ^a, Jan Kroon ^a, Philippe Looten ^b, Pierrick Duflot ^b, Mohamed Mathlouthi ^c^a *Department of Crystal and Structural Chemistry, Bijvoet Center for Biomolecular Research, Utrecht University, Padualaan 8, NL-3584 CH Utrecht, The Netherlands*^b *Roquette Frères, F-62136 Lestrem, France*^c *Faculté des Sciences, Chimie Physique Industrielle, Université de Reims Champagne-Ardenne, Moulin de la Housse BP 1039, F-51687 Reims, France*

Received 9 July 1999; accepted 26 August 1999

Abstract

The crystal structure of maltitol (4-*O*- α -D-glucopyranosyl-D-glucitol) was determined by X-ray diffraction at 95 K and refined to a final conventional parameter of $R = 0.032$. The glucopyranosyl moiety adopts the 4C_1 conformation. The conformation of the glucitol fragment exhibits a [APP(AM)] bent-chain, sickle conformation of the carbon chain. This results in a nearly 1,3-parallel C//O interaction between C-13 and O-16. All hydroxyl groups are involved in a bifurcated entirely intermolecular hydrogen-bond network. © 1999 Elsevier Science Ltd. All rights reserved.

Keywords: X-ray structure; 1,3-Parallel interactions; Conformation; Alditols; Maltitol

1. Introduction

Maltitol is obtained by high-pressure hydrogenation of maltose syrup using a nickel catalyst. Absence of a reducing centre in maltitol gives it high thermal and chemical stability. Many of its physico-chemical properties are comparable to those of sucrose, especially the solubility in water, viscosity of aqueous solutions, hygroscopicity and sweetness potency. Moreover, maltitol has a relatively low energetic value (10.0 kJ/g) and is void of cariogenicity, which permits its use in low-calorie and diet foods.

Comparison of the crystallization behaviour of sucrose and maltitol shows that whereas sucrose remains stable in solution at high supersaturation with a supersolubility curve (limit between metastable and labile regions) at a supersaturation of 1.35, maltitol crystallizes more easily and its metastable limit is situated around a supersaturation of 1.08. Such a difference may originate from the differences in flexibility of the two molecules in concentrated solutions and also from their interactions with water. In supersaturated solutions sucrose adopts a molecular conformation with two intramolecular hydrogen bonds [1] and the same conformation occurs in the crystal structure [2]. In the reported crystal structures of maltitol [3,4], no such hydrogen

* Corresponding author. Fax: +31-30-253-3940.

E-mail address: a.schouten@chem.uu.nl (A. Schouten)

bonds are formed. Moreover, the D-glucitol moiety of maltitol is much more flexible than a pyranose or furanose ring. Establishing and rupturing of hydrogen bonds between maltitol molecules seems to involve less energy than in the case of sucrose. This may be derived from their melting points (146 °C for maltitol and 186 °C for sucrose).

If one assumes that crystallization is a two-step process, diffusion of the hydrated molecule from the bulk of solution to the crystal surface on the one hand and integration of the dehydrated molecule into the crystal on the other, more insight may be gained into the crystallization mechanism. As the viscosities of sucrose and maltitol solutions at

the same concentration and temperature are comparable, the difference in their crystallization mechanisms is certainly due to their interactions with water. In the crystal growth of sucrose, the rate-limiting step is the dissociation of hydration water and its removal in the vicinity of the crystal [5]. This slowness of growth rate favours the formation of large single crystals of sucrose. Oppositely, maltitol molecules easily get rid of their hydration water and show a very high nucleation rate, which prevents one obtaining large single crystals.

To reach accuracy in predicting molecular packing in the steps preceding crystal formation (prenucleation, nucleation), it is necessary for accurate molecular structural data to be available. Although two X-ray structure analyses of maltitol have been reported, we consider a redetermination necessary, because of inconsistencies in both reports, in particular in the description of the hydrogen-bond scheme. The structure reported by Ohno et al. [3] in 1982 contains a wrong position of a hydrogen atom of a hydroxyl group; this has been noted in the Cambridge Structural Database [6]. In the analysis of Park et al. [4] reported in 1989, the above hydrogen position is correct. However, a wrong position of a hydrogen atom of another hydroxyl group is reported and the table of hydrogen bonds is incomplete in that only five hydrogen bonds out of the nine possible ones have been given. This results in a wrong hydrogen-bond scheme.

2. Experimental

A colourless rod-shaped crystal was used for X-ray structural analysis at 95 K. Data were processed using the HKL program package [7]. The structure was solved by direct methods with the program SHELXS-97 [8] and refined on F^2 against all unique reflections with the program SHELXL-97 [9]; the threshold $F > 4\sigma(F)$ was used for calculating $R_{1(\text{obs})}$ only. Intensities were corrected for Lorentz and polarization effects, but not for absorption. The configuration was selected to comply with the known chirality. Crystallographic data of interest are summarized in Table 1.

Table 1
Crystallographic data ^{a,b}

Formula	C ₁₂ H ₂₄ O ₁₁
Molecular weight	344.32
Crystal size (mm)	0.45 × 0.20 × 0.12
Crystal colour	colourless
Crystal system	orthorhombic
Space group	$P2_12_12_1$
Z	4
<i>a</i> (Å)	8.1269(5)
<i>b</i> (Å)	12.6888(8)
<i>c</i> (Å)	13.6581(5)
<i>V</i> (Å ³)	1408.43(13)
<i>D_c</i> (g cm ⁻³)	1.6238(1)
<i>F</i> (000)	736
μ (cm ⁻¹)	1.56
λ (Mo K α) (Å)	0.71073
Temperature of study (K)	95
X-ray exposure time (h)	1.4
$2\theta_{\text{max}}$ (°)	54.95
<i>R</i> _{int} (on F^2)	0.047
Data collection <i>hkl</i> -range	−6 ≤ 10; −14 ≤ 16; −17 ≤ 12
Refinement <i>hkl</i> -range	−10 ≤ 10; 0 ≤ 16; 0 ≤ 17
Reflections measured	9132
Unique reflections (<i>n</i>)	3239 ^f
Reflections with ($F > 4\sigma(F)$)	2968
Number of parameters (<i>p</i>)	235
<i>R</i> _{1(obs)} (on F) ^c	0.032
<i>R</i> _{1(all)} (on F) ^c	0.037
<i>wR</i> _{2(all)} (on F^2) ^d	0.074
Goodness of fit <i>S</i> ^e	1.022
(Δ/σ) _{av3} (Δ/σ) _{max}	0.000, 0.000
$\Delta\rho$ (e Å ⁻³)	−0.20 ≤ 0.26

^a Standard deviations in parentheses.

^b Diffractometer Nonius KappaCCD.

^c $R_1 = \Sigma \|F_o\| - |F_c| / \Sigma |F_o|$.

^d $wR_2 = [\Sigma w(F_o^2 - F_c^2)^2 / \Sigma w(F_o^2)^2]^{1/2}$, $w = 1/[\sigma^2(F_o^2) + (0.0265P)^2 + 0.3755P]$ where $P = (F_o^2 + 2F_c^2)/3$.

^e $S = [\Sigma w(F_o^2 - F_c^2)^2 / (n - p)]^{1/2}$.

^f Reflections belonging to Bijvoet pairs are considered to be independent.

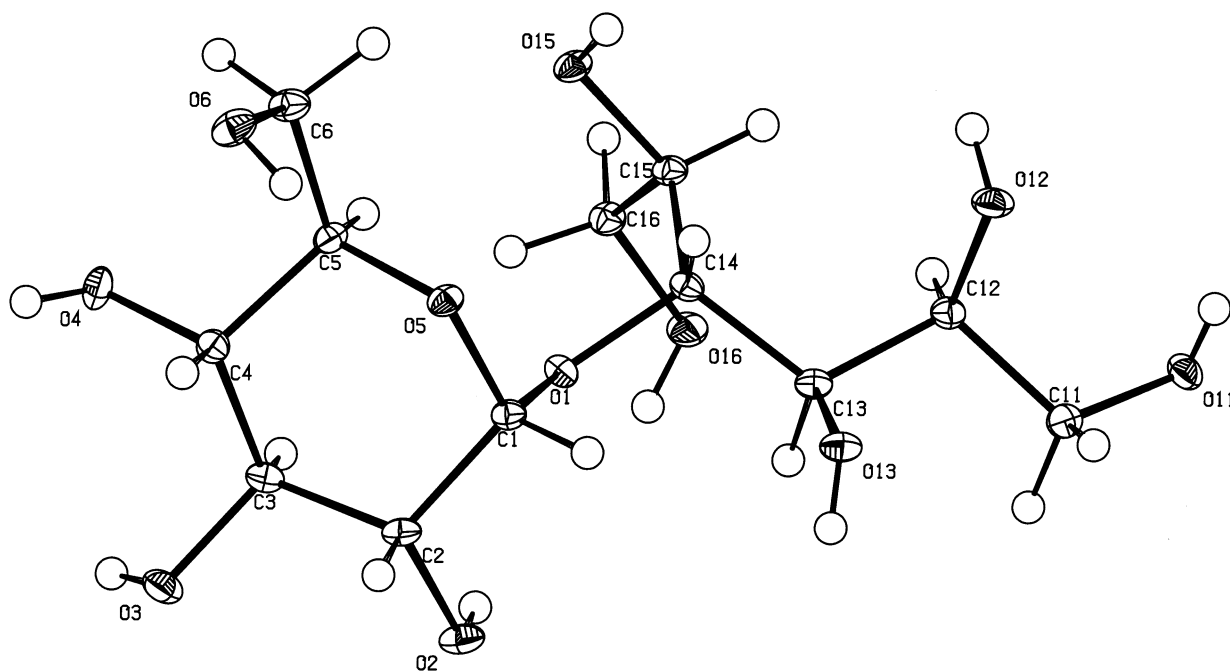


Fig. 1. ORTEP plot of maltitol. Thermal ellipsoids at 50% probability.

The hydroxyl hydrogens were located from difference Fourier maps and were included in the refinement. The non-hydroxyl hydrogens were introduced at theoretical positions and

Table 2

Fractional positional parameters of C and O atoms and equivalent thermal parameters (\AA^2)^a

Atom	<i>x</i>	<i>y</i>	<i>z</i>	<i>U</i> _{eq} ^b
C-1	0.1412(2)	0.4777(1)	0.1110(1)	0.0099(4)
C-2	0.0942(2)	0.4031(1)	0.1951(1)	0.0108(4)
O-2	0.1317(2)	0.4502(1)	0.28736(8)	0.0139(3)
C-3	0.1738(2)	0.2946(1)	0.1851(1)	0.0107(4)
O-3	0.0944(2)	0.2249(1)	0.25239(8)	0.0145(3)
C-4	0.1593(2)	0.2518(1)	0.0808(1)	0.0105(4)
O-4	0.2552(2)	0.15814(9)	0.07220(8)	0.0136(3)
C-5	0.2211(2)	0.3338(1)	0.0079(1)	0.0104(4)
O-5	0.1194(1)	0.42725(9)	0.01854(7)	0.0106(3)
C-6	0.2093(2)	0.2989(1)	−0.0980(1)	0.0130(5)
O-6	0.0499(1)	0.2656(1)	−0.12690(8)	0.0148(3)
C-11	0.4082(2)	0.8850(1)	0.1666(1)	0.0127(4)
O-11	0.5276(2)	0.96883(9)	0.15844(8)	0.0133(3)
C-12	0.4468(2)	0.7917(1)	0.1010(1)	0.0109(4)
O-12	0.4170(2)	0.82322(9)	0.00197(8)	0.0138(3)
C-13	0.3413(2)	0.6975(1)	0.1314(1)	0.0099(4)
O-13	0.1702(1)	0.72825(9)	0.12557(8)	0.0128(3)
C-14	0.3621(2)	0.5976(1)	0.0688(1)	0.0095(4)
O-1	0.3057(1)	0.50806(9)	0.12533(8)	0.0102(3)
C-15	0.5366(2)	0.5726(1)	0.0332(1)	0.0103(4)
O-15	0.5309(1)	0.4961(1)	−0.04460(8)	0.0120(3)
C-16	0.6472(2)	0.5217(1)	0.1096(1)	0.0115(4)
O-16	0.6607(2)	0.5852(1)	0.19631(8)	0.0143(3)

^a Standard deviations in parentheses.

^b $U_{eq} = (\sum_i \sum_j U_{ij} a_i^* a_j^* a_i \cdot a_j) / 3$.

refined riding on their carrier atoms. The last refinement cycles were performed using anisotropic thermal parameters for the non-hydrogen atoms. The hydrogen atoms were assigned constant isotropic thermal parameters equal to the equivalent thermal parameters of their carrier atoms multiplied by a factor of 1.2, except for hydroxyl hydrogens where a factor of 1.5 was used.

3. Results and discussion

A representation of the molecule depicting the thermal ellipsoids is shown in Fig. 1. The program package EUCLID [10] was used for the calculation of geometries and preparation of the illustration. The positional and equivalent isotropic thermal parameters for the non-hydrogen atoms are listed in Table 2 and selected torsion angles are given in Table 3. The glucopyranosyl moiety adopts the 4C_1 conformation. The $[APP(AM)]^1$ bent-chain

¹ *M* = Msc, *P* = Psc and *A* = ap [11] refer to torsion angles of -60° , $+60^\circ$ and 180° , respectively. In order to describe the conformations of the carbon chain as well as those of the terminal hydroxyl groups, the following notation will be used: the first three capitals denote the carbon-chain conformation and the two capitals between parentheses the two terminal OH orientations with respect to the carbon chain.

Table 3
Selected torsion angles (°)^a

Conformation descriptor		
C-11–C-12–C-13–C-14	177.8(1)	<i>A</i>
C-12–C-13–C-14–C-15	37.8(2)	<i>P</i>
C-13–C-14–C-15–C-16	79.1(1)	<i>P</i>
O-11–C-11–C-12–C13	166.4(1)	<i>A</i>
O-12–C-12–C-13–C14	58.1(2)	<i>P</i>
C-11–C-12–C-13–O-13	57.5(1)	<i>P</i>
O-13–C-13–C-14–C-15	158.6(1)	<i>A</i>
C-12–C-13–C-14–O-1	159.1(1)	<i>A</i>
O-1–C-14–C-15–C-16	–42.7(1)	<i>M</i>
C-13–C-14–C-15–O-15	–164.3(1)	<i>A</i>
C-14–C-15–C-16–O-16	–56.8(2)	<i>M</i>
O-11–C-11–C-12–O-12	–71.1(2)	<i>M</i>
O-12–C-12–C-13–O-13	–62.2(1)	<i>M</i>
O-13–C-13–C-14–O-1	–80.0(1)	<i>M</i>
O-1–C-14–C-15–O-15	73.9(1)	<i>P</i>
O-15–C-15–C-16–O-16	–176.9(1)	<i>A</i>

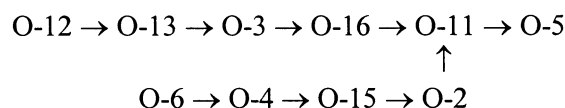
^a Standard deviations in parentheses.

conformation of the glucitol fragment has a nearly parallel C-14–C-13//C-16–O-16 interaction with a distance between C-13 and O-16 of 3.09 Å and a dihedral angle of 15.5°. The molecules are oriented approximately perpendicularly to the *a* axis, and parallel to the *b* axis. The C–C bonds range from 1.516 to 1.538 Å (mean 1.527 Å) and the C–O bonds are in the range 1.405–1.453 Å (mean 1.433 Å). The C–C–C angles range from 109.5 to 116.7° (mean 113.1°) and the C–C–O angles vary from 103.8 to 114.2° (mean 109.4°). The angle in the bridge C-1–O-1–C-14 is 116.2° and the torsion angles about the bridge bonds

are ϕ_1 (O-5–C-1–O-1–C-14) 73.2° and ϕ_2 (C-1–O-1–C-14–C-13) 94.0°, respectively.

The hydrogen-bond geometries are given in Table 4. All nine hydroxyls are involved as donors and, with the exception of O-6–H and O-12–H, as acceptors in an entirely intermolecular hydrogen-bond network. This is compensated for by ring-oxygen O-5, which accepts a hydrogen bond and by O-11, which is a double acceptor. A notable feature is the absence of intramolecular hydrogen bonds.

The bonding sequence consists of bifurcate, finite chains, as shown by the termination of the chains by the ring O-5 acceptor:



When the O–H distances are normalized to 0.97 Å, to correct for the well-known electron displacement from the H nucleus, the H···O distances have a normal range of 1.73–1.96 Å (average 1.85 Å).

4. Supplementary material

Full crystallographic details have been deposited with the Cambridge Crystallographic Data Centre: deposition number 129662. These data may be obtained, on request, from the CCDC, 12 Union Road, Cambridge CB2 1EZ, UK (Tel.: +44-1223-336408; fax: +44-1223-336033; e-mail: deposit@ccdc.cam.ac.uk).

Table 4
Hydrogen-bond geometries (distances in Å, angles in °)^a

Donor–H···Acceptor	Symmetry operation ^b	<i>D</i> – <i>H</i>	<i>H</i> ··· <i>A</i>	<i>D</i> ··· <i>A</i>	<i>D</i> – <i>H</i> ··· <i>A</i>
O-2–H···O-11	4.645	0.80(2)	2.10(2)	2.876(2)	166(1)
O-3–H···O-16	4.645	0.78(3)	1.98(3)	2.756(2)	176(3)
O-4–H···O-15	3.455	0.87(2)	1.83(2)	2.701(2)	177(2)
O-6–H···O-4	3.455	0.85(3)	1.92(2)	2.689(2)	150(2)
O-11–H···O-5	3.565	0.71(3)	2.16(3)	2.853(2)	163(3)
O-12–H···O-13	3.565	0.81(3)	1.98(3)	2.774(2)	171(3)
O-13–H···O-3	4.555	0.79(2)	2.01(2)	2.721(2)	150(2)
O-15–H···O-2	2.564	0.75(3)	2.00(3)	2.735(2)	164(3)
O-16–H···O-11	4.645	0.84(2)	2.08(2)	2.908(2)	166(2)

^a Standard deviations in parentheses.

^b The symmetry operation is performed on the acceptor atom *A*. The first digit indicates one of the following symmetry operations: (1) *x*, *y*, *z*; (2) 0.5–*x*, –*y*, 0.5+*z*; (3) 0.5+*x*, 0.5–*y*, –*z*; (4) –*x*, 0.5+*y*, 0.5–*z*. The last three digits specify the lattice translations, e.g., 4.645 is +*a*–*b* translated from 4.555.

Acknowledgements

The authors thank H. Kooijman for collecting the crystallographic data.

References

- [1] M. Mathlouthi, *Carbohydr. Res.*, 91 (1981) 113–123.
- [2] G.M. Brown, H.A. Levy, *Acta Crystallogr., Sect. B*, 29 (1973) 790–797.
- [3] S. Ohno, M. Hirao, M. Kido, *Carbohydr. Res.*, 108 (1982) 163–171.
- [4] Y.J. Park, J.M. Shin, W. Shin, I. Suh, *Bull. Korean Chem. Soc.*, 10 (1989) 352–356.
- [5] M. Mathlouthi, J. Genotelle, *Carbohydr. Polym.*, 37 (1998) 335–342.
- [6] F.H. Allen, O. Kennard, R. Taylor, *Acc. Chem. Res.*, 16 (1983) 146–153.
- [7] Z. Otwinowski, W. Minor, in C.W. Carter, Jr., R.M. Sweet (Eds.), *Methods Enzymology, Macromolecular Crystallography*, part A, Vol. 276, Academic Press, New York, 1997, pp. 307–326.
- [8] G.M. Sheldrick, SHELXS-97, Program for structure solution, University of Göttingen, Germany, 1997.
- [9] G.M. Sheldrick, SHELXL-97, Program for structure refinement, University of Göttingen, Germany, 1997.
- [10] A.L. Spek, *Acta Crystallogr., Sect. A* 46 (1990) C-34.
- [11] W. Klyne, V. Prelog, *Experientia*, 16 (1960) 521–523.